Computer Aided Geometric Design 102 (2023) 102189

Contents lists available at ScienceDirect

Computer Aided Geometric Design

journal homepage: www.elsevier.com/locate/cagd

Computing the topology of the image of a parametric planar curve under a birational transformation ☆

Juan Gerardo Alcázar [a,*,1,2], Gema M. Diaz-Toca [b,1]

[a] Departamento de Física y Matemáticas, Universidad de Alcalá, E-28871 Madrid, Spain
[b] Departamento de Ingeniería y Tecnología de Computadores, Universidad de Murcia, E-30100 Murcia, Spain

ARTICLE INFO

Article history:
Received 14 October 2022
Received in revised form 3 February 2023
Accepted 22 March 2023
Available online 28 March 2023

Keywords:
Computation of the topology of a planar curve
Birational mappings
Algorithms
Parametric curves
Planar rational curves
Planar analytic curves

ABSTRACT

We provide a method to compute the topology of the image of a parametric curve under a birational mapping of the plane. The method proceeds by exploiting as much as possible the initial parametrization in order to reduce the computational cost. The self-intersections of the image curve are derived from points in the image where the inverse of the birational mapping is not defined. In order to compute these points, we prove a result characterizing birational planar mappings, together with an algorithm to compute the inverse of a birational mapping. We apply the method when the original curve is rational, in which case the image of the curve is also rational but with a higher degree, and when the original curve is an *exp-log-arctan* function. In this last case the image is a non-rational curve admitting an analytic parametrization, a problem not treated in the literature so far.

1. Introduction

In the context of Computational Algebraic Algebra, the computation of the topology of a curve is the computation of a graph isotopic to the curve, therefore showing its main topological features. This problem, both for planar and space curves, has received continued attention for more than thirty years: from seminal papers like Arnon and MacCallum (1988); El Kahoui and González-Vega (1996); González-Vega and Necula (2002); Hong (1996) to more recent algorithms like Berberich et al. (2013); Diatta et al. (2022), the problem has been addressed by many authors, many of which appear in the bibliographies of Berberich et al. (2013); Diatta et al. (2022). Furthermore, typically the algorithms for solving this problem require to isolate roots of univariate polynomials and of bivariate polynomial systems, which has stimulated greatly the research on these fundamental questions.

The same problem for parametric curves has not received so much attention, and up to our knowledge there are only two main references: Alcázar and Díaz Toca (2010) and Katsamaki et al. (2020), which improves on the algorithm in Alcázar and Díaz Toca (2010). A potential explanation for this lack of references is the fact that visualizing a parametric curve is certainly easier, from a computational point of view, compared to the implicit case: while in the implicit case one needs to

☆ Editor: Ron Goldman.

* Corresponding author.
E-mail addresses: juange.alcazar@uah.es (J.G. Alcázar), gemadiaz@um.es (G.M. Diaz-Toca).

1 Authors are partially supported by the grant PID2020-113192GB-I00/AEI/10.13039/501100011033 (Mathematical Visualization: Foundations, Algorithms and Applications) from the Spanish State Research Agency (Ministerio de Ciencia e Innovación).

2 Member of the Research Group ASYNACS (Ref. CCEE2011/R34).

https://doi.org/10.1016/j.cagd.2023.102189

compute the values of the polynomial defining the curve on a grid (Mudiyanselage et al., 2022), in the parametric case it suffices to evaluate the components of the parametrization on a real interval.

However, and this is when the algorithms to compute the topology are useful, on the one hand visualizing the curve requires to know in advance a box defining the region of the plane where the curve is to be plotted: in the parametric case, this box is deduced from a real interval where the parameter should take values in order to reproduce the main features of the curve. On the other hand, the plotting of the curve can be tricky sometimes, and its topological behavior may not be easily readable from the plotting. In the case of parametric curves, this can happen, although not only, when the real interval to plot the curve contains values generating a branch at infinity of the curve.

In this paper the objective is not the computation of the topology of a rational curve, that can be efficiently done with the algorithm in Katsamaki et al. (2020), but of the topology of the curve resulting after applying a birational transformation of the plane to a given parametric curve. Easy examples of these transformations are affine, projective or Möbius planar transformations, but birational planar mappings can be much more complicated. In Algebraic Geometry these mappings commonly receive the name of *Cremona transformations* (Hudson and Reid, 2011), and are known to be generated from projective linear transformations and standard quadratic transformations. In general, applying these mappings increases the degree and the coefficient size of the original parametrization, and as a consequence the parametrization of the image curve can be much bigger. Roughly, if we consider a parametrization of degree n, i.e. n is the biggest power appearing in the numerators and denominators of the parametrization, and a birational planar mapping of degree N, then after applying the birational mapping the image parametrization has degree $\mathcal{O}(Nn)$. This results in higher computation times or even the failure of the machine to compute the topology.

For these reasons, in this paper we present an alternative algorithm to compute the topology of such an image, which exploits as much as possible the original parametrization together with the equations of the birational mapping.

Our strategy is as follows. Computing the topology requires finding first the vertices of a graph isotopic to the curve, that must be connected afterwards. In the case of parametric curves, the most difficult part is finding the vertices. Among the vertices we have singularities and ramification points, i.e. points where the tangent is vertical, plus other points that are easier to find. In our case, we avoid using the parametrization obtained after the birational mapping to compute the singularities of the image, which is the most costly part, and the ramification points of the image. In particular, we use the inverse of the birational mapping, computed by means of an algorithm also provided in this paper, to find the self-intersections of the image curve. The main idea to do this, inspired by Alcázar et al. (2020), is that the inverse of the birational mapping is not defined at the self-intersections of the image curve which do not come from self-intersections of the original curve: therefore, computing the parameter values where this happens provides a superset for the parameter values generating self-intersections of the image. For finding the remaining vertices of the graph we are looking for, i.e. vertices which are neither singularities nor ramification points of the image, that do not require so much computation effort, we use the parametrization of the image.

We apply our ideas when the original curve is rational, in which case the image curve is also rational, and also when the original curve has the form $y = f(t)$ where $f(t)$ is an *exp-log-arctan* function (Strzebónski, 2012). These functions are analytic functions in a closed class having finitely many real roots (Strzebónski, 2012). After applying a birational planar mapping to such a curve we get a parametric, not rational curve. Thus, our algorithm can also serve to compute the topology of non-algebraic curves defined by analytic parametrizations whenever they can be written this way, i.e. as the composition of a birational mapping and an analytic function of the considered kind. This enlarges the class of curves whose topology we can compute, which in the literature reduces so far to algebraic curves, either parametrically or implicitly defined. The topology of curves $y = f(t)$ is very simple; thus, our algorithm just needs to compute the potential changes in the topology of $y = f(t)$ introduced by the birational mapping (e.g. self-intersections, branches at infinity, etc.)

The complexity of the algorithm in Katsamaki et al. (2020), which assumes that the coefficients of the parametrization are rational numbers, is thoroughly analyzed in Katsamaki et al. (2020), and yields complexity bounds analogous to the best complexity bounds known for implicit curves. We do not provide here a complexity analysis of our algorithm, and at the present stage it is not clear if such an analysis would provide a bound different from Katsamaki et al. (2020). However, in practice, the fact of working with curves of smaller degrees and coefficients can make a difference. In this paper we provide several examples of curves whose topology cannot be computed with the current implementation of Alcázar and Díaz Toca (2010) and Katsamaki et al. (2020), but can, however, be computed with our algorithm very quickly. For curves involving exp-log-arctan functions, complexity results are very difficult to obtain and so far, up to our knowledge, there have been no contributions in this direction.

The structure of this paper is the following. We motivate the problem in Section 2, where we also provide some background, as well as the general strategy to solve it. Section 3 is devoted to developing an algorithm, using resultants, to compute the inverse of a planar birational mapping. The method to solve the problem is given in Section 4, where we also provide examples, first for the case when the original curve is rational, and then for graphs of *exp-log-arctan* functions, carried out with `Maple 2021`, and, in the case of *exp-log-arctan* functions, also with the help of `Mathematica`; the implementation for the rational case can be downloaded from Toca (2022). We close with our conclusion in Section 5, where we also suggest several problems to continue the same line of research. The proofs of the results in Section 3 are given in Appendix A, so as to improve the readability of the paper. Details on the curves used in our experimentation are provided in Appendix B.

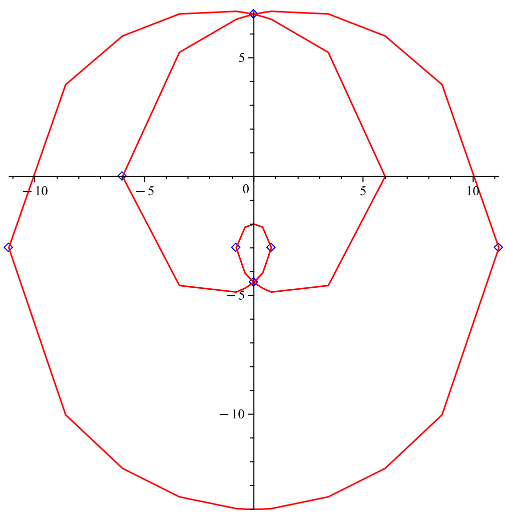

Fig. 1. Curve corresponding to Eq. (1).

Acknowledgments: We thank the reviewers of the paper for their comments, which helped to improve the previous version of the paper.

2. Motivation of the problem, preliminaries and strategy

2.1. Motivation

Consider the rational planar curve $\mathcal{C} \subset \mathbb{R}^2$ (an offset of the cardioid curve) defined by means of the parametrization $\boldsymbol{x}(t) = (x(t), y(t))$, where

$$\begin{aligned} x(t) &= \frac{6t^8 - 756t^6 + 3456t^5 - 31104t^3 + 61236t^2 - 39366}{t^8 + 36t^6 + 486t^4 + 2961t^2 + 6561}, \\ y(t) &= \frac{-18t(6t^6 - 16t^5 - 126t^4 + 864t^3 - 1134t^2 - 1296t + 4374)}{t^8 + 36t^6 + 486t^4 + 2961t^2 + 6561}, \end{aligned} \tag{1}$$

which is depicted in Fig. 1, taken from Alcázar and Díaz Toca (2010). Since the highest power of the parameter t appearing in the numerators and denominators of $x(t), y(t)$ is 8, we will say that this parametrization has degree 8. Furthermore, the biggest coefficient appears in the numerator of $y(t)$ and is equal to 78732, so the maximum of the absolute values of the coefficients is $\approx 2^\tau$ with $\tau = 17$, i.e. the bitsize of the coefficients in $\boldsymbol{x}(t)$ is bounded by $\tau = 17$.

Now consider the planar mapping $\Pi : \mathbb{R}^2 \to \mathbb{R}^2$, where $\Pi = \phi \circ \psi$, with

$$\phi(x, y) = \left(\frac{x}{x^2 + y^2}, \frac{y}{x^2 + y^2}\right), \ \psi(x, y) = \left(\frac{x + y + 1}{x}, \frac{x - y}{x}\right).$$

Here one can recognize the composition of a projective linear transformation, ψ, and an inversion from the origin, ϕ. Since both ϕ, ψ are birational, Π is also a birational transformation of the plane of degree two, i.e.

$$\Pi(x, y) = \left(\frac{x(x + y + 1)}{2x^2 + 2y^2 + 2x + 2y + 1}, \frac{(x - y)x}{2x^2 + 2y^2 + 2x + 2y + 1}\right). \tag{2}$$

The image $\Pi(\mathcal{C})$ of $\mathcal{C}$ under the birational mapping Π is an also rational curve defined by a parametrization $\boldsymbol{y}(t)$ of degree 16, where the biggest coefficient is $8401649184 \approx 2^{33}$, i.e. both the degree and the bitsize have doubled after applying Π. Thus, if we want to compute a picture similar to Fig. 1 using algorithms like Alcázar and Díaz Toca (2010); Katsamaki et al. (2020), we have to work with a parametrization of high degree and high coefficients, which results in a more expensive computational cost. In fact, the available implementation of the algorithm in Katsamaki et al. (2020) could not compute the topology of $\Pi(\mathcal{C})$ after 60 seconds, when we stopped the computation, with the machine used in the experimentation of this paper (iMac, chip M1 Apple, CPU with 8 kernels, GPU with 4 kernels, neural engine with 16 kernels, 16 Gbytes of memory). The analysis of the topology of $\Pi(\mathcal{C})$ will be carried out in Section 4 (see Example 1).

Our goal in this paper is to provide an algorithm to compute the topology of the image $\Pi(\mathcal{C})$ of a parametric planar curve $\mathcal{C}$, properly parametrized (i.e. generically injective) by $\boldsymbol{x}(t) = (x(t), y(t))$, under a birational planar mapping $\Pi : \mathbb{R}^2 \to \mathbb{R}^2$,

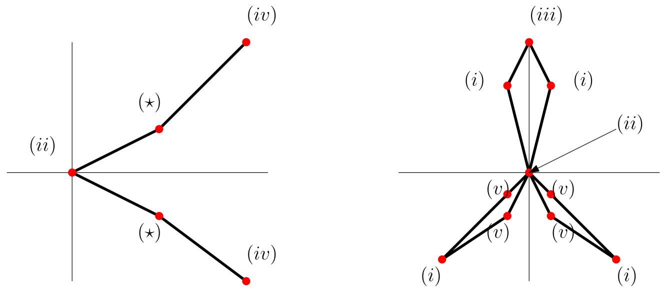

Fig. 2. Graphs associated to the cubic cusp, and the three-leaved rose.

reducing the use of the parametrization $\boldsymbol{y}(t) = \Pi(\boldsymbol{x}(t))$ to the minimum and using instead the information provided by the mapping Π itself, and the original parametrization $\boldsymbol{x}(t)$. We will consider rational parametrizations and also certain non-rational parametrizations. In the next subsections we recall how to capture the topology of a rational curve, we address non-rational curves of a special type, and we finally present the overall strategy.

2.2. Topology of a planar rational curve

The topology of a planar rational curve $\mathcal{C}$ is represented by means of a graph $\mathcal{G}_{\mathcal{C}}$, isotopic to the curve. Assuming that $\mathcal{C}$ is given by means of a proper rational parametrization, the vertices of $\mathcal{G}_{\mathcal{C}}$ are:

(i) The *ramification* points of $\mathcal{C}$, i.e. the points where $x'(t) = 0$.
(ii) The *singular points* of $\mathcal{C}$, which include two different types of points: the *local singularities*, corresponding to the points where $x'(t) = y'(t) = 0$ (for instance, cusps), and the *self-intersections* of the curve, corresponding to the points where $\boldsymbol{x}(t) = \boldsymbol{x}(s)$ with $t \neq s$.
(iii) The point $p_\infty = \lim_{t\to\infty}\boldsymbol{x}(t)$, when it is affine, which can be a point of $\mathcal{C}$ not reached by any affine value of t.
(iv) *Endpoints* for non-bounded branches of $\mathcal{C}$, if any, including branches corresponding to vertical asymptotes, which must be computed as well.
(v) The points of $\mathcal{C}$ lying in the vertical lines defined by the points in (i-iv); this is not essential to compute the graph, but it guarantees that the edges of the resulting graph intersect only at self-intersections, and helps to get a better understanding, from $\mathcal{G}_{\mathcal{C}}$, of the topology of $\mathcal{C}$.

Furthermore, two vertices of $\mathcal{G}_{\mathcal{C}}$ are connected by an edge of $\mathcal{G}_{\mathcal{C}}$ whenever there is a branch of $\mathcal{C}$ connecting the points of $\mathcal{C}$ giving rise to the vertices. In order to draw the graph, one computes the t-values $t_1, \dots, t_p$ generating the vertices, plus the points $\boldsymbol{x}(t_i) = (x(t_i), y(t_i))$, with $i \in \{1, \dots, p\}$, themselves. We also include as vertices of $\mathcal{G}_{\mathcal{C}}$ the points of $\mathcal{C}$ lying on each vertical line $x = x(t_i)$ in order to improve the appearance of the graph. Although not always necessary, one can also add as vertices the points of $\mathcal{C}$ lying in vertical lines in between two consecutive verticals $x = x(t_i)$, again to provide some more detail on how the curve looks like. After computing the vertices, one has a box $B \subset \mathbb{R}^2$ (called a *characteristic box* in Katsamaki et al. (2020), since it captures the topological features of $\mathcal{C}$) which represents the topology of $\mathcal{C} \cap B$ and corresponds to the points of $\boldsymbol{x}(t)$ with $t \in I$, where $I \subset \mathbb{R}$ is an interval containing the values t_i, $i = 1, \dots, p$. Finally, the vertices are connected according to the order in the t_i, i.e. if the t-values of the vertices are

$$-\infty < t_1 < \cdots < t_p < +\infty,$$

we connect each $\boldsymbol{x}(t_i)$ with $\boldsymbol{x}(t_{i+1})$.

We provide two examples of graphs in Fig. 2, corresponding to the cubic cusp, that is parametrized by $\boldsymbol{x}(t) = (t^2, t^3)$, and the three-leaved rose, parametrized by

$$\boldsymbol{x}(t) = \left(\frac{t(t^2-3)}{t^4+2t^2+1}, \frac{t^2(t^2-3)}{t^4+2t^2+1}\right).$$

In Fig. 2 we have labeled the vertices of each graph according to the type of vertex $(i - v)$, from the enumeration before. Furthermore, the vertices labeled with $(\star)$ are additional vertices, not essential to compute the graph, which are provided to improve its appearance and correspond to points of the curve in between two vertical lines defined by vertices $(i - v)$. The plottings of the curves, computed with Maple's command `plot_real_curve`, are provided in Fig. 3.

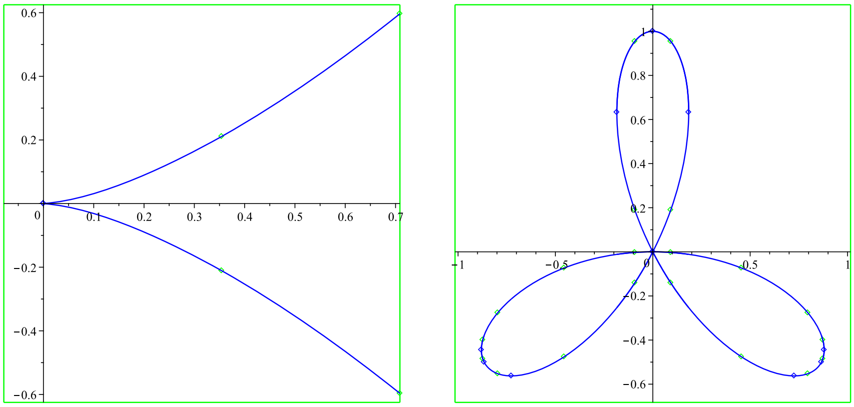

Fig. 3. Plottings of the cubic cusp and the three-leaved rose.

2.3. Topology of a planar non-rational curve

In this paper we will also consider curves $\mathcal{C}$ of the type $y = f(t)$, where $f(t)$ is an *exp-log-arctan* function. An exp-log-arctan function $f(t)$ is, quoting (Strzebónski, 2012), *the smallest set of partial real functions containing* exp, log, arctan, *the identity function and the constant functions that is closed under addition, multiplication and composition of functions.*

One can see that the set of these functions contains the rational functions, as well as radical functions, inverses of trigonometric functions, hyperbolic functions and inverses of hyperbolic functions (see also Strzebónski, 2012), and is closed under differentiation. Furthermore, again quoting (Strzebónski, 2012), *the domain of an* exp-log-arctan *function consists of a finite number of open, possibly unbounded, intervals and an* exp-log-arctan *function has a finite number of real roots.* Algorithms to compute the domain and the real roots of these functions exist, and are implemented, for instance, in `Mathematica`. The computer algebra system `Maple` also has some commands for computing with analytic functions, but some functionalities are still missing.

So we will also consider the case of a curve $\mathcal{C}$ parametrized by $\boldsymbol{x}(t) = (t, f(t))$, with $f(t)$ an exp-log-arctan function, and its image $\Pi(\mathcal{C})$ under a birational planar mapping Π. Thus, $\Pi(\mathcal{C})$ is parametrized by $\boldsymbol{y}(t) = \Pi(t, f(t))$, whose components are rational functions of $t, f(t)$. Here $t \in D(f)$, where $D(f)$ is the *domain* of $f(t)$. The only difference with respect to Subsection 2.2 is that here $D(f)$ is not necessarily equal to $\mathbb{R}$ minus a finite set of points; otherwise, it can be a finite union of intervals, so the images for the extremes of these intervals must be also included as vertices of the graph.

2.4. Strategy

In order to compute the graph $\mathcal{G}_{\Pi(\mathcal{C})}$ one needs to determine the vertices and edges of this graph. For the rational case, the complexity analysis (cf. Katsamaki et al., 2020) shows that the bottleneck of the computation is the computation of singularities, both local and global, i.e. self-intersections. Thus our strategy will be:

(1) Compute the ramification points and the singularities of $\Pi(\mathcal{C})$ making use of the original parametrization $\boldsymbol{x}(t)$, and the birational planar mapping Π itself, i.e. without making use of the parametrization $\boldsymbol{y}(t)$ of $\Pi(\mathcal{C})$. In more detail:
- For ramification points and local singularities, we will use the *Jacobian* of Π (see Section 4).
- For self-intersections, we will make use of both the self-intersections of the original curve and the inverse Π^{-1} of Π (see Section 3 and Section 4), taking advantage of the fact that at the self-intersections of $\Pi(\mathcal{C})$ which are not the image of a self-intersection of $\mathcal{C}$, the inverse Π^{-1} is not defined; we will also take into account that these singularities can be generated by branches at infinity, or base points of Π belonging to $\mathcal{C}$.

(2) For the rest of the computation, we will use $\boldsymbol{y}(t) = \Pi(\boldsymbol{x}(t))$.

Since each vertex is generated by some t-value(s), connecting the vertices comes for free by just following the t-values generating the vertices in increasing order.

3. Inverse of a birational planar transformation

Let $\Pi : \mathbb{R}^2 \to \mathbb{R}^2$ be the rational mapping

$$\Pi(x, y) = (u, v) = (\Pi_1(x, y), \Pi_2(x, y)) = \left(\frac{A(x, y)}{B(x, y)}, \frac{C(x, y)}{D(x, y)}\right), \tag{3}$$

with A, B and C, D relatively prime. We say that Π is *birational* if it has a rational inverse Π^{-1},

$$\Pi^{-1}(u,v) = (x,y) = (\Pi_1^{-1}(u,v), \Pi_2^{-1}(u,v)) = \left(\frac{M(u,v)}{N(u,v)}, \frac{P(u,v)}{Q(u,v)}\right). \tag{4}$$

Remark 1.

(i) Π^{-1} exists and is affine for $(u,v) \in \mathbb{C}^2 \backslash \mathcal{M}$, where $\mathcal{M}$ is an at most 1-dimensional subset of $\mathbb{C}^2$ defined by $N(u,v) \cdot Q(u,v) = 0$. That is, there is an at most 1-dimensional subset of points of $\mathbb{C}^2$ where the inverse is not defined or is not an affine point. In particular, the equality $\Pi \circ \Pi^{-1} = \Pi^{-1} \circ \Pi = \mathrm{id}_{\mathbb{C}^2}$ holds over all the complex plane with the exception of an at most 1-dimensional subset.

(ii) A point (x_0, y_0) such that $A(x_0,y_0) = B(x_0,y_0) = 0$ (resp. $C(x_0,y_0) = D(x_0,y_0)$) is called a *base point* of $\Pi_1(x,y)$ (resp. $\Pi_2(x,y)$). Since A, B and C, D are relatively prime, the number of base points of either Π_i is finite. A base point of Π is a point which is a base point of both Π_1, Π_2. Although Π is not defined at base points of Π_1, Π_2, sometimes we will write $\Pi(x_0,y_0) = (u_0,v_0)$ at a base point (x_0,y_0) of Π_i to mean that the limit of $\Pi(x,y)$ for $(x,y) \to (x_0,y_0)$ along some path exists, and is equal to (u_0,v_0).

(iii) A birational mapping Π can map a whole curve to a point; for instance, $\Pi(x,y) = (x, xy)$ maps the line $x=0$ to the origin. However, the number of curves where this happens must be finite. The reason is that by definition, Π is birational if and only if Π^{-1} is birational; then we just apply observation (i) to the inverse of Π^{-1}, which is Π. Notice that this is not true if the mapping is not birational. For instance, $\Pi(x,y) = (x+y, (x+y)^2)$ maps every line $x+y=k$, with k a constant, to the point (k,k^2); in fact, this mapping maps the whole plane to a curve, namely a parabola.

(iv) If some Π_i is constant then Π cannot be birational, because Π^{-1} is only defined over a line. Also, if both Π_i depend just on x or just on y then Π cannot be birational either, because Π^{-1} is only defined over a curve. Thus, we will assume that Π is not that way.

Our goal in this section is to provide an algorithm to compute Π^{-1}. There are certainly different alternatives to perform this computation, all of them based on elimination. For instance, Gröbner bases can be used. Also, one can see $\Pi(x,y)$ as a proper parametrization of a plane, for instance the plane $z=0$, and then apply the algorithm in Pérez-Díaz et al. (2002) to invert the parametrization. The algorithm in Pérez-Díaz et al. (2002) uses resultants, so it is more efficient than the one using Gröbner bases. However, the algorithm in Pérez-Díaz et al. (2002) is essentially devised for more complicated surfaces, other than planes, involves computations over the field of rational functions of the surface, and may require a linear change of coordinates to satisfy certain hypotheses. Thus, here we will present an approach, which certainly resembles that of Pérez-Díaz et al. (2002) although adapted to our case, to solve the problem also using resultants, whose structure is described. The proofs of the results in this section are provided in Appendix A so as to improve the readability of the paper.

For now we will assume that both Π_i depend on x and y; we will treat the case when at least one Π_i depends on just one variable at the end of the section. Now, let

$$F_1(x,y,u) = uB(x,y) - A(x,y),\ F_2(x,y,v) = vD(x,y) - C(x,y).$$

Also, let $I = \langle F_1, F_2 \rangle$ be the ideal in $\mathbb{C}[x,y,u,v]$ generated by F_1, F_2, and let $\mathcal{U} = \mathcal{V}(I) \subset \mathbb{C}^4$ the variety of the ideal I, consisting of the $(x_0,y_0,u_0,v_0) \in \mathbb{C}^4$ such that $F_1(x_0,y_0,u_0) = F_2(x_0,y_0,v_0) = 0$. Then $\mathcal{U}$ is the union of four different sets:

(1) The points $(x_0,y_0,u_0,v_0) \in \mathcal{U}$ such that $B(x_0,y_0) \neq 0$ and $D(x_0,y_0) \neq 0$. Thus, here (x_0,y_0) is not a base point of either Π_i. These points satisfy that $\Pi(x_0,y_0) = (u_0,v_0)$. We represent the set consisting of these points by U_1.

(2) The points $(x_0,y_0,u_0,v_0) \in \mathcal{U}$ with $A(x_0,y_0) = B(x_0,y_0) = 0$ and $D(x_0,y_0) \neq 0$. Thus, (x_0,y_0) is a base point of Π_1 but not of Π_2. Here $v_0 = \Pi_2(x_0,y_0)$, and u_0 can take any value in $\mathbb{C}$, so the set of these points, which we denote by U_2, corresponds to a 1-dimensional component of $\mathcal{U}$.

(3) The points $(x_0,y_0,u_0,v_0) \in \mathcal{U}$ with $C(x_0,y_0) = D(x_0,y_0) = 0$ and $B(x_0,y_0) \neq 0$. Thus, (x_0,y_0) is a base point of Π_2 but not of Π_1. Here, $u_0 = \Pi_1(x_0,y_0)$ and v_0 can take any value in $\mathbb{C}$, so the set of these points, which we denote by U_3, also corresponds to a 1-dimensional component of $\mathcal{U}$.

(4) The points $(x_0,y_0,u_0,v_0) \in \mathcal{U}$ with $A(x_0,y_0) = B(x_0,y_0) = C(x_0,y_0) = D(x_0,y_0) = 0$. Here (x_0,y_0) is a base point of both Π_1, Π_2 and (u_0,v_0) can take any value in $\mathbb{C}^2$. Thus, the set of these points, which we denote by U_4, corresponds to a 2-dimensional component of $\mathcal{U}$.

Therefore, we have

$$\mathcal{U} = U_1 \cup U_2 \cup U_3 \cup U_4. \tag{5}$$

Additionally, let

$$\xi_1(x,u,v) = \mathrm{Res}_y(F_1,F_2),\ \xi_2(y,u,v) = \mathrm{Res}_x(F_1,F_2). \tag{6}$$

Since by hypothesis A, B and C, D are relatively prime, so are F_1, F_2, and therefore ξ_1, ξ_2 are not identically zero.

Let $\mathcal{V}(\xi_1), \mathcal{V}(\xi_2)$ be the varieties in $\mathbb{C}^3$ defined by ξ_1, ξ_2. These varieties are non-empty because $U_1 \neq \emptyset$ and, by Lemma 7.3.2 of Mishra (1993), if $(x_0, y_0, u_0, v_0) \in U_1$ then $(x_0, u_0, v_0) \in \mathcal{V}(\xi_1)$ and $(y_0, u_0, v_0) \in \mathcal{V}(\xi_2)$. As a consequence, ξ_1, ξ_2 are not constant polynomials.

In order to clarify the relationship between $\mathcal{V}(\xi_1), \mathcal{V}(\xi_2)$ and $\mathcal{U}$, we need to introduce some more notation. Let

$$\begin{aligned} h_1 &= h_1(x,u) = \mathrm{lc}_y(F_1), \quad h_2 = h_2(x,v) = \mathrm{lc}_y(F_2), \\ j_1 &= j_1(y,u) = \mathrm{lc}_x(F_1), \quad j_2 = j_2(y,v) = \mathrm{lc}_x(F_2), \end{aligned} \tag{7}$$

be the leader coefficients of F_1, F_2 with respect to y, x. Notice that $\gcd(h_1, h_2)$ (resp. $\gcd(j_1, j_2)$) is either 1 or a univariate polynomial $\alpha(x)$ (resp. $\beta(y)$). Furthermore, let $\mathcal{V}(h_1, h_2)$ (resp. $\mathcal{V}(j_1, j_2)$) be the variety in $\mathbb{C}^3$ consisting of the points where both h_1, h_2 (resp. j_1, j_2) vanish. Observe that $\mathcal{V}(h_1, h_2)$ is empty iff some h_i is constant; if $\mathcal{V}(h_1, h_2)$ is not empty, $\mathcal{V}(h_1, h_2)$ consists of the union of 2-dimensional components corresponding to the planes $x = x_i$ defined by the roots of $\alpha(x)$ and another component, if any, $\mathcal{V}^\star(h_1, h_2)$, of dimension at most 1. Similarly for $\mathcal{V}(j_1, j_2)$. Moreover, the following result, which essentially follows from Extension Theorem, see Corollary 7, Chapter 3, Section 6 of Cox et al. (1992), holds.

Proposition 1. *The following statements hold:*

(1) If $(x_0, u_0, v_0) \in \mathbb{C}^3$ is a zero of $\xi_1(x, u, v)$ satisfying that $(x_0, u_0, v_0) \notin \mathcal{V}(h_1, h_2)$, then there exists $y_0 \in \mathbb{C}$ such that $(x_0, y_0, u_0, v_0) \in \mathcal{U}$.
(2) If $(y_0, u_0, v_0) \in \mathbb{C}^3$ is a zero of $\xi_2(y, u, v)$ satisfying that $(y_0, u_0, v_0) \notin \mathcal{V}(j_1, j_2)$, then there exists $x_0 \in \mathbb{C}$ such that $(x_0, y_0, u_0, v_0) \in \mathcal{U}$.

Proposition 1 is essential to prove the following results on the structure of $\xi_1(x, u, v)$ and $\xi_2(y, u, v)$. In order to examine this structure, let us write

$$\xi_1(x,u,v) = V_1(x) \cdot V_2(u) \cdot V_3(v) \cdot V_4(x,u) \cdot V_5(x,v) \cdot V_6(u,v) \cdot V_7(x,u,v), \tag{8}$$

where V_4 (resp. V_5 and V_6) explicitly depends on both x, u (resp. x, v and u, v), and V_7 explicitly depends on the three variables x, u, v. We assume here that V_4, V_5, V_6 do not have univariate factors, and that V_7 does not have univariate or bivariate factors. Similarly, we write

$$\xi_2(y,u,v) = W_1(y) \cdot W_2(u) \cdot W_3(v) \cdot W_4(y,u) \cdot W_5(y,v) \cdot W_6(u,v) \cdot W_7(x,u,v), \tag{9}$$

The next lemma, proven in Appendix A, sheds some light on some of the roots of $V_1(x)$ and $W_1(y)$.

Lemma 2. *If x_0 (resp. y_0) is either a root of $\alpha(x)$ (resp. $\beta(y)$) or the x-coordinate (resp. the y-coordinate) of a base point of both Π_1, Π_2, then $V_1(x_0) = 0$ (resp. $W_1(y_0) = 0$).*

Moreover, we have the following three lemmas, whose proofs can also be found in Appendix A.

Lemma 3. *Under our assumptions, V_2, V_3 (resp. W_2, W_3) must be constant and nonzero.*

Lemma 4. *Under our assumptions, V_4, V_5 (resp. W_4, W_5) must be constant and nonzero.*

The previous lemmata do not require that Π is birational. The next two, however, do require it.

Lemma 5. *Under our assumptions, if Π is birational then V_6 (resp. W_6) must be constant and nonzero.*

Lemma 6. *Under our assumptions, if Π is birational then V_7 (resp. W_7) cannot be constant.*

Finally, we arrive at the following theorem, also proven in Appendix A, which allows us both to check whether or not Π is birational, and to compute Π^{-1} in the affirmative case. Here we denote the square-free parts of V_7, W_7 by $\widehat{V}_7, \widehat{W}_7$.

Theorem 7. *Assume that no Π_i is constant, or depends just on x or just on y. The mapping Π is birational if and only if*

$$\xi_1(x,u,v) = V_1(x)V_7(x,u,v), \; \xi_2(y,u,v) = W_1(y)W_7(y,u,v), \tag{10}$$

where $\widehat{V}_7, \widehat{W}_7$ are powers of a linear polynomial in x, y respectively, i.e.

$$\widehat{V}_7(x,u,v) = xN(u,v) - M(u,v), \; \widehat{W}_7(y,u,v) = yQ(u,v) - P(u,v). \tag{11}$$

Furthermore, if Π is birational then

$$\left(\frac{M(u,v)}{N(u,v)}, \frac{P(u,v)}{Q(u,v)}\right)$$

is the inverse Π^{-1}.

Notice that V_1, W_1 can be computed as

$$V_1 = \text{Content}_v(\text{Content}_u(\xi_1)),\ W_1 = \text{Content}_v(\text{Content}_u(\xi_2)). \tag{12}$$

Thus, we get the algorithm `Inverse` to check the birationality and compute the inverse of a mapping $\Pi(x, y)$.

Algorithm 1 Inverse.

Require: A mapping $\Pi(x, y) = (\Pi_1(x, y), \Pi_2(x, y))$, where each Π_i is not constant and depends both on x and y.
Ensure: Whether or not $\Pi(x, y)$ is birational, and the inverse mapping $\Pi^{-1}(u, v)$ in the affirmative case.
1: Compute the resultants $\xi_1(x, u, v)$, $\xi_2(y, u, v)$ in Eq. (6).
2: Compute $V_1(x), W_1(y)$ by means of Eq. (12)
3: Compute the factor $V_7(x, u, v)$ by dividing $V_1(x)$ out of $\xi_1(x, u, v)$, and its square-free part $\widehat{V}_7(x, u, v)$.
4: Compute the factor $W_7(y, u, v)$ by dividing $W_1(y)$ out of $\xi_2(y, u, v)$, and its square-free part $\widehat{W}_7(y, u, v)$.
5: **if** $\widehat{V}_7(x, u, v)$ is linear in x and $\widehat{W}_7(y, u, v)$ is linear in y **then**
6: Solve $\widehat{V}_7(x, u, v) = 0$ for x, and solve $\widehat{W}_7(y, u, v) = 0$ for y.
7: **return** `The mapping is birational`, plus the inverse $\Pi^{-1}(u, v)$, whose components are the two expressions computed in the step before.
8: **else**
9: **return** `The mapping is not birational.`
10: **end if**

Finally, we consider the case where some of component of Π depends only on one variable. Thus, let us assume that one of the Π_i depends just on one variable, say $\Pi_1(x, y) = \Pi_1(x)$. Since $\Pi^{-1} \circ \Pi$ is the identity, Π_1^{-1} only depends on u, and therefore Π defines a birational transformation of the real line. As a consequence, Π must be a Möbius transformation, i.e.

$$\Pi_1(x) = \frac{\alpha x + \beta}{\gamma x + \delta},\ \alpha\delta - \beta\gamma \neq 0.$$

Notice that in order to find Π_2^{-1}, the only possibility is that F_2 is linear in y. Thus, whenever one of the components depends on just one variable, say x, such component must be a Möbius transformation, and the other component must be a rational function in x, y where the numerator and the denominator have degree at most one in y.

3.1. Birationality of a rational map on a curve

Now we consider a curve $\mathcal{C}$ defined by a parametrization $\boldsymbol{x}(t) = (x(t), y(t))$, and we wonder when the restriction $\Pi|_{\mathcal{C}}$, Π being a birational planar mapping, is birational itself. This happens when:

(i) Π is defined at almost all points of $\mathcal{C}$, i.e. with the exception of finitely points of $\mathcal{C}$.
(ii) The inverse Π^{-1} is defined at almost all points of $\Pi(\mathcal{C})$.

In order to check (i), we just need to verify whether or not some denominator in Eq. (3), i.e. $B(x, y)$ or $D(x, y)$, entirely vanishes when substituting $x := x(t)$, $y := y(t)$. To check (ii), we do the same with $\boldsymbol{y}(t) = \Pi(\boldsymbol{x}(t))$ and Eq. (4), i.e. we check whether $N(u, v)$ or $Q(u, v)$ entirely vanishes when substituting u, v by the components of $\boldsymbol{y}(t)$.

In particular, if $\Pi|_{\mathcal{C}}$ is birational then no branch of $\mathcal{C}$ collapses to a point when Π is applied, and no branch of $\Pi(\mathcal{C})$ collapses to a point when Π^{-1} is applied. In the rest of the paper, we will restrict ourselves to this case.

4. Computation of the topology of $\Pi(\mathcal{C})$

4.1. Rational curves

Let $\mathcal{C} \subset \mathbb{R}^2$ be a rational curve, defined by means of a rational parametrization

$$\boldsymbol{x}(t) = (X(t), Y(t)) = \left(\frac{x(t)}{w(t)}, \frac{y(t)}{w(t)}\right) \tag{13}$$

where $\gcd(x(t), y(t), w(t)) = 1$. Furthermore, let $\Pi : \mathbb{R}^2 \to \mathbb{R}^2$ as in Eq. (3) be a birational planar mapping.

In order to find the topology of $\Pi(\mathcal{C})$ we must find the points enumerated in Subsection 2.2. Before that, observe that the Jacobian matrix of Π, J_Π, maps tangent vectors to $\mathcal{C}$ onto tangent vectors to $\Pi(\mathcal{C})$. Thus, if $\boldsymbol{x}'(t)$ is well-defined and $J_\Pi(\boldsymbol{x}(t))$ denotes the Jacobian matrix of Π at the point $p = \boldsymbol{x}(t)$, applying the Chain rule we have that

$$J_{\Pi}(\boldsymbol{x}(t)) \cdot \boldsymbol{x}'(t) \tag{14}$$

is tangent to $\Pi(\mathcal{C})$ at the point $\Pi(p)$.

Now we can list the points of $\Pi(\mathcal{C})$ that we must compute. In fact, from Subsection 2.4 what we really need are the t-parameters of the points of $\mathcal{C}$ giving rise to the points and branches we are going to enumerate. Joining these points is, unlike the implicit case, easy: once the t-parameters of these points are known, we connect them by increasing t, as explained in Subsection 2.2. To this list of points we need to add the points generated in $\Pi(\mathcal{C})$ by base points of Π belonging to $\mathcal{C}$, which we will discuss later.

(1) *Ramification points of* $\Pi(\mathcal{C})$*:* they correspond to points where the first component of the vector in Eq. (14) vanishes.
(2) *Local singularities of* $\Pi(\mathcal{C})$*:* they correspond to points where the vector in Eq. (14) is entirely zero.
(3) *Self-intersections of* $\Pi(\mathcal{C})$*:* they correspond to either the images under Π of the self-intersections of $\mathcal{C}$, which can be computed from the parametrization $\boldsymbol{x}(t)$, or to the points generated by t-values for which Π^{-1} cannot be found. From Eq. (3) and Eq. (4), such t-values are among the roots of
$$N(\Pi(\boldsymbol{x}(t)))\,Q\,(\Pi(\boldsymbol{x}(t))). \tag{15}$$
(4) *Points not reached by the parametrization:* here we must compute
$$\lim_{t\to\infty}\Pi(\boldsymbol{x}(t)).$$
If p_∞ is affine and Π is well defined at p_∞, by the continuity of Π the above limit is equal to $\Pi(p_\infty)$. This point can be either a regular point or a singularity of $\Pi(\mathcal{C})$.
(5) *Non-bounded branches of* $\Pi(\mathcal{C})$*:* they correspond to the t-values such that some denominator of $\Pi(\boldsymbol{x}(t))$ is zero.

Furthermore, if $\mathcal{C}$ contains points which are base of points of Π, their behavior must be analyzed. If $P = \boldsymbol{x}(t_0)$ is such a point, then this amounts to studying

$$\lim_{t\to t_0}\Pi(\boldsymbol{x}(t)).$$

If this limit is a real point, then it is added as a vertex of the graph of $\Pi(\mathcal{C})$. If the limit is $\pm\infty$, then we have a branch of $\Pi(\mathcal{C})$ at infinity.

The following example, where we complete the study of the curve that served us to motivate the problem in Section 2.1, illustrates these ideas.

Example 1. Let us consider the curve $\mathcal{C}$ parametrized as in Eq. (1), and the mapping $\Pi : \mathbb{R}^2 \to \mathbb{R}^2$ in Eq. (2). The inverse Π^{-1} is, using the algorithm in Section 3,

$$\Pi^{-1}(u,v) = \left(-\frac{u^2+v^2}{2u^2+2v^2-u-v}, -\frac{u^2+v^2-v}{2u^2+2v^2-u-v}\right).$$

Thus, according to the notation in Eq. (4),

$$N(u,v) = Q\,(u,v) = 2u^2+2v^2-u-v. \tag{16}$$

Next, ramification and local singularities of $\Pi(\mathcal{C})$ generated by points of $\mathcal{C}$, leaving aside points of $\mathcal{C}$ which are base points of Π, are generated by t-values which are roots of the first component of Eq. (14). In our case, these t-values, rounded to three significant digits, are

$$\begin{gathered} -56.426,\ -10.006,\ -4.855,\ -2.584,\ -1.319,\\ -0.496,\ 0.246,\ 1.605,\ 4.646,\ 11.047. \end{gathered} \tag{17}$$

The self-intersections of $\Pi(\mathcal{C})$, leaving aside points of $\mathcal{C}$ which are base points of Π, are generated by t-values which are roots of Eq. (15), with the N, Q in Eq. (16), and the $\boldsymbol{x}(t)$ in Eq. (1). The list of these t-values, rounded to three significant digits, is:

$$-12.951, -3., -0.695, 1.162, 3., 7.745 \tag{18}$$

Denoting the two self-intersections of $\mathcal{C}$ (see Fig. 1) by $\mathbf{p}_1, \mathbf{p}_2$, where $\mathbf{p}_1$ has a positive y-coordinate and $\mathbf{p}_2$ has a negative y-coordinate (the x-coordinate of both $\mathbf{p}_1$, $\mathbf{p}_2$ is zero), one can see that the first and third elements in Eq. (18) generate $\mathbf{p}_1$, while the fourth and sixth elements in Eq. (18) generate $\mathbf{p}_2$.

There is a point of $\mathcal{C}$ not generated by $\boldsymbol{x}(t)$, i.e. corresponding to $t = \pm\infty$, namely $p_\infty = (6, 0)$. This point generates the point $\Pi(p_\infty) = \left(\frac{42}{85}, \frac{36}{85}\right)$, belonging to $\Pi(\mathcal{C})$. Finally, Π has one base point, namely $\left(-\frac{1}{2}, -\frac{1}{2}\right)$, but this point does not belong to $\mathcal{C}$.

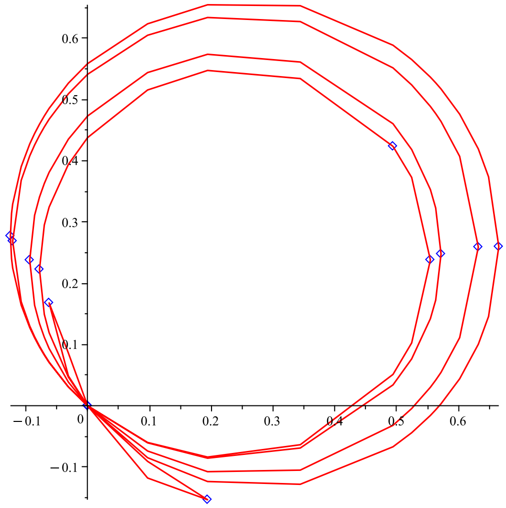

Fig. 4. Image of the curve in Eq. (1) under the birational mapping in Eq. (2). (For interpretation of the colors in the figure(s), the reader is referred to the web version of this article.)

Table 1
Rational curves.

Ex.	d_x	τ_x	d_Π	d_y	τ_y	Time
2	4	7	8	32	56	0.993
3	3	1	10	22	7	1.396
4	8	5	2	16	10	4.629
5	4	7	8	24	46	0.296
6	6	18	8	32	102	1.992
7	8	5	2	16	12	2.999

Therefore, we include as vertices of the graph associated with $\Pi(\mathcal{C})$ the points $\Pi(\boldsymbol{x}(t_i))$ where t_i appears in Eq. (17) and Eq. (18), plus the point $\Pi(p_\infty)$. These points are connected by edges by increasing t, taking into account that the points generated by the smallest and highest t-values in Eq. (17) or Eq. (18) must also be connected with $\Pi(p_\infty)$. Some extra vertices are computed to improve the appearance of the graph, which is shown in Fig. 4. We plot in blue the vertices of the graph corresponding to singularities and ramification points of $\Pi(\mathcal{C})$, as well as $\Pi(p_\infty)$. Here one can see that all the points of $\mathcal{C}$ on the line $x=0$, in particular both self-intersections of $\mathcal{C}$, are mapped to the unique self-intersection of $\Pi(\mathcal{C})$, at the origin. The whole computation took 1.252 seconds in the machine specified in Subsection 2.1.

We provide now six more examples computed with our method, implemented in the computer algebra system `Maple 2021`. The information on these examples is summarized in Table 1, where we show, in order, the number of each example, the degree $d_{\boldsymbol{x}}$ of the parametrization $\boldsymbol{x}(t)$ of $\mathcal{C}$, an upper bound $\tau_{\boldsymbol{x}}$ on the bitsizes of the coefficients in $\boldsymbol{x}(t)$, the degree d_Π of the birational mapping Π, the degree $d_{\boldsymbol{y}}$ of the parametrization $\boldsymbol{y}(t)=\Pi(\boldsymbol{x}(t))$, an upper bound $\tau_{\boldsymbol{y}}$ on the bitsizes of the coefficients in $\boldsymbol{y}(t)$, and the timing, in seconds, for computing the topology of the curve defined by $\boldsymbol{y}(t)$ using our method; the details on the curves appear in Appendix B. In Table 1 we can see that the degree of the original parametrization has a direct influence on the timing, even more than the degree of the birational mapping. The outputs for these examples can be found in Fig. 5. We plot in blue the vertices of the graphs corresponding to singularities and ramification points of the image of the curve under the considered birational mapping, as well as $\Pi(p_\infty)$, when $p_\infty, \Pi(p_\infty)$ are affine. In all the cases the execution of the algorithm in Katsamaki et al. (2020) to directly compute the topology of the curve defined by $\boldsymbol{y}(t)$ was stopped after 60 seconds, as it also happened with Example 1, without obtaining an output.

We would like to end this section by mentioning that the implementation can be downloaded from Toca (2022). The `Maple` procedure that a user must use to obtain the graph is called `grafo` and, at the beginning of the file, the input parameters are described in detail.

4.2. Non-rational curves

Here we consider curves $\mathcal{C}\subset\mathbb{R}^2$ of the type $y=f(t)$ where $f(t)$ is an exp-log-arctan function, and we address the topology of $\Pi(\mathcal{C})$, where Π is a birational transformation of the plane. Therefore, $\Pi(\mathcal{C})$ is a non-algebraic, parametric curve parametrized by $\boldsymbol{y}(t)=\Pi(t,f(t))$. The strategy for these curves is the same strategy of Subsection 4.1. However, here the domain of t is the domain of the function f, which needs to be computed. In order to do this we used `Mathematica`,

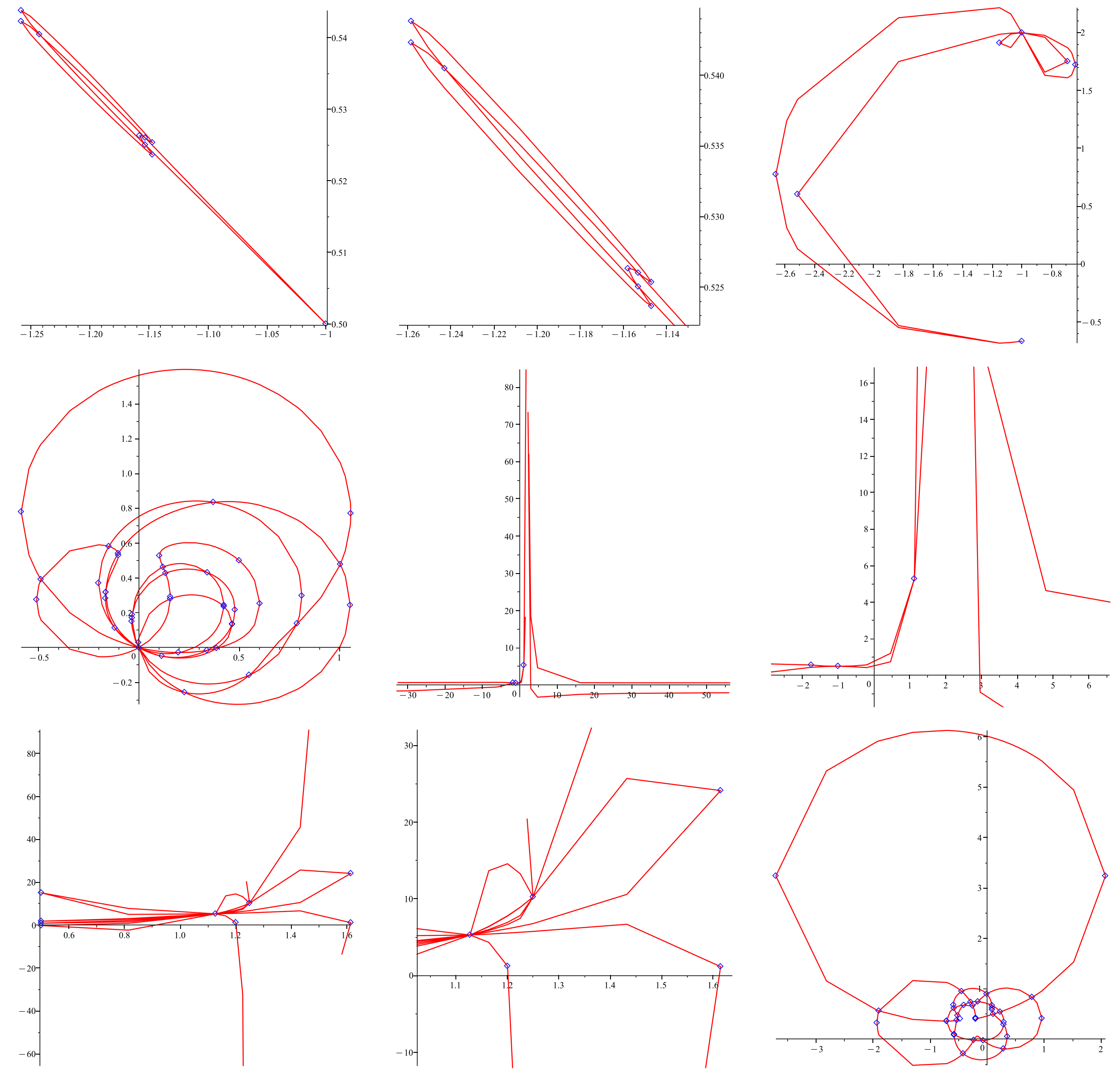

Fig. 5. Examples of the algorithm for rational curves: upper row Ex. 2 (left), detail of Ex. 2 (middle), Ex. 3 (right); medium row Ex. 4 (left), Ex. 5 (middle), detail of Ex. 5 (right); bottom row Ex. 6 (left), detail of Ex. 6 (middle), Ex. 7 (right).

since `Maple` still does not have a command to find the domain. Additionally, we used the Maple's command `RootFinding[Analytic]` to compute the (finitely many) roots of exp-log-arctan functions. However, this command requires to know an interval to look for these roots, which must be found by the user in advance, for instance plotting the function. An alternative method is, again, using `Mathematica`, where there is a similar command to compute the roots of an analytic function that does not require any interval.

In Fig. 6 we provide six examples of these curves, which were computed using both `Maple` and `Mathematica` (for the domains and the roots of the functions); the details can be found in Appendix B. All these curves are images of $y = f_i(t)$, with

$$f_1(t) = e^t, \;\; f_2(t) = \frac{t^3 - e^t}{\log(t)}$$

under different birational mappings. Since the resulting curves are not algebraic, here we observe topologies that cannot arise in the algebraic realm. That is the case of the first and last examples, where we have points where the plot abruptly ends, and also points (in fact, self-intersections of the image) with two “coming” branches and just one “leaving” branch.

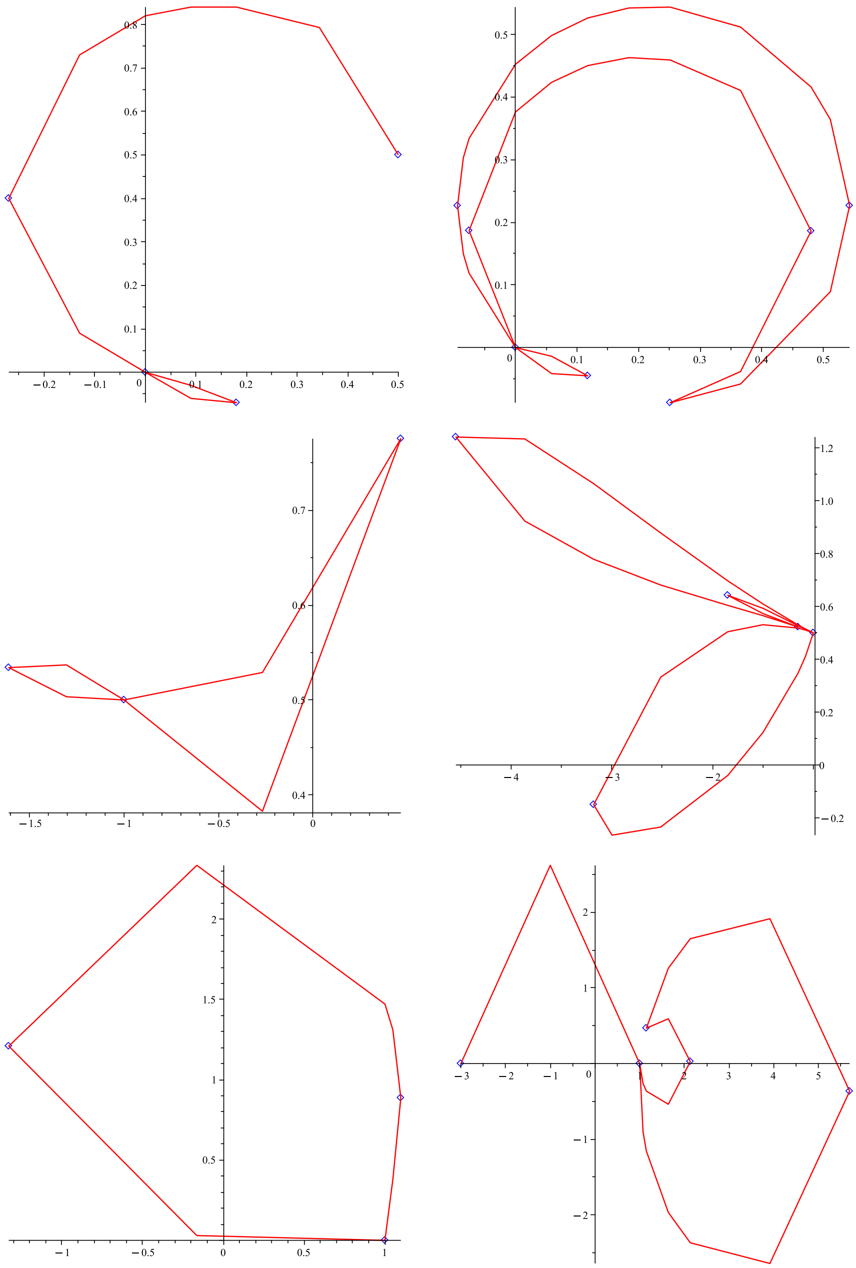

Fig. 6. Examples of the algorithm for non-rational curves: upper row Ex. 8 (left), Ex. 9 (right); medium row Ex. 10 (left), Ex. 11 (right); bottom row Ex. 12 (left), Ex. 13 (right).

5. Conclusion and further work

We have addressed the computation of the topology of the image of a parametric curve under a birational transformation of the plane. The initial curve can be either a rational curve, in which case the image is also rational, or an exp-log-arctan function, in which case the image is not rational. Although the first case can also be approached with existing algorithms, the performance of these algorithms can be either slower, or just non-successful. The key idea is to exploit as much as possible the parametrization of the initial curve, and use the inverse of the birational transformation to compute the self-intersections of the image, which is the most costly part in any algorithm to compute the topology.

An interesting question, not addressed in this paper, is the computation of the topology of the image of a given curve under a transformation which is not birational on the whole plane, but is birational on the curve. However, the difficulty in this case is how to efficiently compute the inverse of the restriction to the curve.

Another natural continuation of the research in this paper is to address implicit planar curves. This problem seems to admit a similar analysis although the analysis of certain points, e.g. base points, may require to use Puiseux series. Other directions are the generalization of the results to 3D curves, which in turn requires to address the computation of the inverse of a transformation in three variables, and the computation of the intersection of an implicit surface and a parametric surface, that in the generic case can be approached, again, as the three dimensional image of a planar curve under a birational map.

CRediT authorship contribution statement

Juan Gerardo Alcázar: theoretical part, reading, writing. **Gema M. Díaz-Toca:** theoretical part, reading, implementation.

Declaration of competing interest

The authors declare the following financial interests/personal relationships which may be considered as potential competing interests:

Juan Gerardo Alcazar Arribas reports financial support was provided by Spain Ministry of Science and Innovation.

Data availability

A link to the code is provided in the paper. Data used in the experiments are also provided in the paper.

Appendix A. Proof of the results in Section 3

Here we provide the proofs of the lemmas and theorems in Section 3. We begin with Lemma 2.

Proof of Lemma 2. We prove it for $V_1(x)$; for $W_1(y)$, the proof is analogous. By the Sylvester form of the resultant, $\alpha(x)$ divides $V_1(x)$, so any root of $\alpha(x)$ is also a root of $V_1(x)$. Now if x_0 is the x-coordinate of a base point (x_0, y_0) of both Π_1, Π_2, then $F_1(x_0, y_0, u) = F_2(x_0, y_0, v) = 0$ for any $(u, v) \in \mathbb{C}^2$. By well-known properties of the resultant Mishra (1993), (x_0, u, v) is a zero of ξ_1 for any $(u, v) \in \mathbb{C}^2$, so $V_1(x_0) = 0$. □

Now we prove Lemma 3.

Proof of Lemma 3. We prove the result for $V_2(u)$; for $V_3(v), W_2(u), W_3(v)$ the proofs are analogous. Assume by contradiction that $V_2(u)$ is not a constant polynomial, and let $u_0 \in \mathbb{C}$ satisfy that $V_2(u_0) = 0$. Additionally, let $(x_0, v_0) \in \mathbb{C}^2$ such that:

(i) x_0 is not either a root of $V_1(x)$ or the x-coordinate of a base point of some Π_i; notice that almost all x_0 satisfy this because under our assumptions, the number of base points of each Π_i is finite.
(ii) The image of $x = x_0$ under the mapping Π, that we denote by $\mathcal{C}_{x_0}$ and is defined by $\Pi(x_0, y)$ (i.e. is a rational curve) is not the line $u = u_0$. Notice that since Π_1 is not a constant, Π cannot contract the whole plane onto the line $u = u_0$, so almost all x_0 satisfy this.
(iii) $(u_0, v_0) \notin \mathcal{C}_{x_0}$. Again, since $\Pi(x_0, y)$ is not the line $u = u_0$, almost all v_0 satisfy this.
(iv) $(x_0, u_0, v_0) \notin \mathcal{V}(h_1, h_2)$; notice that for a given u_0 there are always infinitely many (x_0, v_0) such that $V_1(x_0) \neq 0$ and $(x_0, u_0, v_0) \notin \mathcal{V}(h_1, h_2)$.

Since $V_2(u_0) = 0$, the point (x_0, u_0, v_0) is a zero of ξ_1. Thus, by Proposition 1 there exists $y_0 \in \mathbb{C}$ such that $(x_0, y_0, u_0, v_0) \in \mathcal{U}$. Since x_0 is not the x-coordinate of a base point of some Π_i, (x_0, y_0, u_0, v_0) does not belong to either U_2, or U_3, or U_4, so $(x_0, y_0, u_0, v_0) \in U_1$. But this cannot happen either because $(u_0, v_0) \notin \mathcal{C}_{x_0}$, and therefore we cannot have $\Pi(x_0, y_0) = (u_0, v_0)$, which is the condition satisfied by the points in U_1. Thus, we reach a contradiction, so the lemma is proven. □

In order to prove Lemma 4 we need a preliminary result.

Lemma 8. *Let $\Pi(x, y)$ be a mapping as in Eq. (3), not necessarily birational, with $A(x, y), B(x, y)$ and $C(x, y), D(x, y)$ relatively prime polynomials, such that neither A/B nor C/D are constant or depend on just one variable.*

(1) There are just finitely many $(x_0, u_0) \in \mathbb{C}^2$ such that $\Pi_1(x_0, y) - u_0$ is identically zero.
(2) There are just finitely many $(x_0, v_0) \in \mathbb{C}^2$ such that $\Pi_2(x_0, y) - v_0$ is identically zero.

Proof. We will prove (1); the proof of (2) is analogous. We prove it by contradiction. Assume that (1) is not true, so that there are infinitely many (x_0, u_0) such that $\Pi_1(x_0, y) - u_0$ is identically zero. Notice that this last condition implies that $F_1(x_0, y, u_0) = 0$ for all y. Now let us write

$$F_1(x,y,u) = a_n(x,u)y^n + a_{n-1}(x,u)y^{n-1} + \cdots + a_0(x,u).$$

Since A, B depend explicitly on y, we have that $n \geq 1$. If there are infinitely many (x_0, u_0) with $F_1(x_0, y, u_0) = 0$, the curves in the (x, u) plane defined by $a_i(x, u) = 0$ have infinitely many points in common. Thus, all the $a_i(x, u)$ must have a nontrivial common factor $\ell(x, u)$, which is also a factor of $F_1(x, y, u)$. Since $F_1(x, y, u) = uB(x, y) - A(x, y)$, either $A(x, y)$ is identically zero, which is excluded by hypothesis, or there exists a common factor of $B(x, y)$ and $A(x, y)$. However, this cannot happen either because by hypothesis A, B are relatively prime. Thus, we get a contradiction, so (1) is true. □

Now we can prove Lemma 4.

Proof of Lemma 4. We prove the result for $V_4(x, u)$; for $V_5(x, v)$, $W_4(y, u)$, $W_5(y, v)$ the proofs are analogous. Assume that $V_4(x, u)$ is not constant, and let $(x_0, u_0) \in \mathbb{C}^2$ with $V_4(x_0, u_0) = 0$ such that:

(i) x_0 is not either a root of $V_1(x)$, or the x-coordinate of a base point of some Π_i; notice that almost all x_0 satisfy this, because by hypothesis $V_4(x, u)$ does not have univariate factors.
(ii) $\Pi_1(x_0, y) - u_0$ is not identically zero; observe that by Lemma 8, almost all (x_0, u_0) satisfy this.

Additionally, let $v_0 \in \mathbb{C}$ such that

(a) $(u_0, v_0) \notin \mathcal{C}_{x_0}$, where $\mathcal{C}_{x_0}$ is the curve in the (u, v) plane (maybe a line at infinity) defined by $\Pi(x_0, y)$. Notice that since $\Pi_1(x_0, y) - u_0$ is not identically zero, $\mathcal{C}_{x_0}$ is not the line $u = u_0$, so almost all v_0 satisfy this.
(b) $(x_0, u_0, v_0) \notin \mathcal{V}(h_1, h_2)$: since $V_1(x_0) \neq 0$ almost all v_0 satisfy $(x_0, u_0, v_0) \notin \mathcal{V}(h_1, h_2)$.

Since $V_4(x_0, u_0) = 0$, the point (x_0, u_0, v_0) is a zero of ξ_1, and by Proposition 1 there must exist $y_0 \in \mathbb{C}$ such that $(x_0, y_0, u_0, v_0) \in \mathcal{U}$. However, arguing as in the proof of Lemma 3, we conclude that there does not exist $k \in \{1, 2, 3, 4\}$ with $(x_0, y_0, u_0, v_0) \in U_k$, which is a contradiction. □

Now let us prove Lemma 5.

Proof of Lemma 5. We prove the result for $V_6(u, v)$; for $W_6(u, v)$ the proof is analogous. Assume that $V_6(u, v)$ is not constant, and let $(u_0, v_0) \in \mathbb{C}^2$. Furthermore, let $x_0 \in \mathbb{C}$ which is not either a root of $V_1(x)$ or the x-coordinate of a base point of some Π_i, and such that $(x_0, u_0, v_0) \notin \mathcal{V}(h_1, h_2)$; notice that almost all values of x_0 satisfy this. Since $V_6(u_0, v_0) = 0$, the point (x_0, u_0, v_0) is a zero of ξ_1. Thus, since $(x_0, u_0, v_0) \notin \mathcal{V}(h_1, h_2)$, by Proposition 1 there must exist $y_0 \in \mathbb{C}$ such that $(x_0, y_0, u_0, v_0) \in \mathcal{U}$. Since $\mathcal{U} = U_1 \cup U_2 \cup U_3 \cup U_4$ and x_0 is not the x-coordinate of a base point of some Π_i, $(x_0, y_0, u_0, v_0) \in U_1$, i.e. $\Pi(x_0, y_0) = (u_0, v_0)$. However, keeping our choice of (u_0, v_0), we reach the same conclusion for any other $x_0^\star$ fulfilling the same conditions as x_0. Thus, we conclude that there exists a curve $\mathcal{C}_0$ such that $\Pi(\mathcal{C}_0) = \{(u_0, v_0)\}$, so $\mathcal{C}_0$ collapses to the point (u_0, v_0) when Π is applied. Taking any other point $(u_0^\star, v_0^\star) \in \mathbb{C}^2$ with $V_6(u_0^\star, v_0^\star) = 0$, we also deduce that there exists a curve $\mathcal{C}_0^\star$ such that $\Pi(\mathcal{C}_0^\star) = \{(u_0^\star, v_0^\star)\}$. Since the curve defined by $V_6(u, v) = 0$ in the (u, v) plane contains infinitely many points, we conclude that there are infinitely many curves collapsing to a point when Π is applied. However, if Π is birational, this is impossible (see statement (iii) in Remark 1). □

Notice that Lemma 5 *does* require the mapping Π to be birational: for instance, the mapping $\Pi(x, y) = (x + y, (x + y)^2)$, which is not birational, satisfies that $\xi_1(x, u, v) = v - u^2$. In fact, as observed in Remark 1, this mapping contracts infinitely many lines to points of the plane (compare with the final argument in the proof of Lemma 5). We proceed now with Lemma 6.

Proof of Lemma 6. We prove the result for V_7; similarly for W_7. Assume by contradiction that V_7 is constant. By Lemma 3, Lemma 4 and Lemma 5, $\xi_1(x, u, v) = V_1(x)$. Now let x_0 satisfy that: (i) $V_1(x_0) \neq 0$; (ii) $x - x_0$ is not a factor of either $B(x, y)$ or $D(x, y)$. Also, let (u_0, v_0) be a point of the rational curve in the (u, v) plane defined by $\Pi(x_0, y)$, and let y_0 such that $\Pi(x_0, y_0) = (u_0, v_0)$. Then $(x_0, y_0, u_0, v_0) \in \mathcal{U}$, and therefore $\xi_1(x_0) = 0$. But this cannot happen because $V_1(x_0) \neq 0$ by hypothesis. □

Finally we can prove Theorem 7.

Proof of Theorem 7. ($\Rightarrow$) The structure of ξ_1, ξ_2 in Eq. (10) is a consequence of the lemmata previously proven in this appendix. Thus, let us see that $\widehat{V}_7, \widehat{W}_7$ are linear in x, y respectively. We prove it for $\widehat{V}_7$; for $\widehat{W}_7$ the proof is analogous. Let $(u_0, v_0) \in \mathbb{C}^2$ satisfy the following conditions:

(1) Π^{-1} is defined at (u_0, v_0), so that (u_0, v_0) is the image under Π of just one point (x_0, y_0). That is, $\Pi(x_0, y_0) = (u_0, v_0)$ and $\Pi^{-1}(u_0, v_0) = (x_0, y_0)$.

(2) (u_0, v_0) does not belong to any curve $\widehat{V_7}(\bar{x}, u, v) = 0$, defined in the (u, v) plane, with $\bar{x}$ a root of $V_1(x)$, or the x-coordinate of a base point of some Π_i.
(3) The polynomial $\widehat{V}_7(x, u_0, v_0)$ is square-free.
(4) The leading coefficient of $\widehat{V}_7(x, u, v)$ with respect to x does not vanish at (u_0, v_0).
(5) (u_0, v_0) does not belong to the projection onto the (u, v) plane of the component $\mathcal{V}_1^\star(h_1, h_2)$ of $\mathcal{V}(h_1, h_2)$ of dimension at most 1.

Observe that almost all points (u_0, v_0) satisfy these conditions, i.e. there is at most a 1-dimensional set of points in the (u, v) plane not satisfying conditions (1-5).

Consider now $\gamma(x) = \widehat{V}_7(x, u_0, v_0)$. First, notice that $\deg(\gamma(x)) \geq 1$. Indeed, because of condition (1) there exists (x_0, y_0) such that $\Pi(x_0, y_0) = (u_0, v_0)$, so $(x_0, y_0, u_0, v_0) \in \mathcal{U}$, and therefore $\xi_1(x_0, u_0, v_0) = 0$. Since from condition (2) we have $V_1(x_0) \neq 0$, we deduce that x_0 is a root of $\gamma(x)$, and hence $\deg(\gamma(x)) \geq 1$.

Let us see that, in fact, $\deg(\gamma(x)) = 1$. Since x_0 is not a multiple root of $\gamma(x)$ because of condition (3), if $\deg(\gamma(x)) > 1$ then there must exist another root x_1 of $\gamma(x)$, so (x_1, u_0, v_0) is also a zero of ξ_1. By conditions (2) and (5) $(x_1, u_0, v_0) \notin \mathcal{V}(h_1, h_2)$, so by Proposition 1 there exists y_1 such that $(x_1, y_1, u_0, v_0) \in \mathcal{U}$. Additionally, again by condition (2) we have $(x_1, y_1, u_0, v_0) \in U_1$, i.e. $\Pi(x_1, y_1) = (u_0, v_0)$. However, because of condition (1) this implies that $x_0 = x_1$. Hence, $\deg(\gamma(x)) = 1$.

Finally, by condition (4), the degree of $\widehat{V}_7(x, u, v)$ in x is equal to $\deg(\gamma(x))$, so we deduce that $\widehat{V}_7(x, u, v)$ is linear in x.

($\Leftarrow$) Since V_7, W_7 are powers of linear polynomials in x, y, we can solve x, y in terms of u, v to get

$$x = f_1(u, v) = \frac{M(u, v)}{N(u, v)}, y = f_2(u, v) = \frac{P(u, v)}{Q(u, v)}),$$

where $f_1(u, v)$ and $f_2(u, v)$ are rational functions. For a generic choice of (u, v), the points

$$\left(\frac{M(u, v)}{N(u, v)}, u, v\right), \ \left(\frac{P(u, v)}{Q(u, v)}, u, v\right)$$

are zeroes of ξ_1, ξ_2, respectively, and are lifted, by Proposition 1, to points in $\mathcal{U}$ belonging to U_1. Thus, (u, v) is the image of $(x, y) = (f_1(u, v), f_2(u, v))$ under Π, so $(f_1(u, v), f_2(u, v))$ is the inverse Π^{-1} of Π. Since Π has a rational inverse, Π is birational. $\square$

Appendix B. Details on the curves used in Section 4

In this appendix we provide more information on the rational and non-rational curves appearing in Fig. 5 and Fig. 6.

Rational curves: (Fig. 5 in Subsection 4.1).

Example 2:

$$\boldsymbol{x}(t) = \left(-40t^2 + 20 + \frac{130t^4}{3}, 32t - \frac{136t^3}{3}\right), \ \Pi(x, y) = (\Pi_1(x, y), \Pi_2(x, y)),$$

$$\Pi_1(x, y) = \frac{-x^2 - y^2 - 2x}{x^2 + y^2 - x},$$

$$\Pi_2(x, y) = \frac{x^8 + 4x^6y^2 + 6x^4y^4 + 4x^2y^6 + y^8 - x^5y - 2x^3y^3 - xy^5 + x^4 - 2x^3y}{(2x^6 + 6x^4y^2 + 6x^2y^4 + 2y^6 - 2x^5 - 4x^3y^2 - 2xy^4 + x^2y)(x^2 + y^2)}.$$

Example 3:

$$\boldsymbol{x}(t) = (t^2, t^3), \ \Pi(x, y) = \left(\frac{A(x, y)}{B(x, y)}, \frac{C(x, y)}{D(x, y)}\right),$$

$A(x, y) = -x^{10} - 9 + (4y + 2)x^9 - 4(y + 1/2)^2x^8 + (-2y - 8)x^7 + (7y^2 + 16y + 22)x^6 +$
$(-8y^2 - 38y - 20)x^5 + (-y^2 + 64y + 2)x^4 + (-2y^2 - 42y - 16)x^3 + (-y^2 + 8y + 35)x^2 +$
$(-6y - 6)x,$

$B(x, y) = 9 + x^{10} + (-4y - 2)x^9 + 4(y + 1/2)^2x^8 + (2y + 8)x^7 + (5y^2 - 16y - 22)x^6 +$
$(-4y^2 - 10y + 20)x^5 + (y^2 + 32y + 46)x^4 + (2y^2 - 6y - 128)x^3 + (y^2 - 8y + 109)x^2 +$
$(6y - 42)x,$

$C(x, y) = -6 + 2x^{10} + (-8y - 4)x^9 + (8y^2 + 12y + 2)x^8 + (-8y^2 - 4y + 8)x^7 +$
$(18y^2 - 12y - 20)x^6 + (-4y^2 - 36y + 16)x^5 + (2y^2 + 28y + 68)x^4 + (36y - 136)x^3 +$
$2(y - 5)^2x^2 + (4y + 20)x,$

$D(x, y) = 9 + x^{10} + (-4y - 2)x^9 + 4(y + 1/2)^2x^8 + (2y + 8)x^7 + (5y^2 - 16y - 22)x^6 + (-4y^2 - 10y + 20)x^5 + (y^2 + 32y + 46)x^4 + (2y^2 - 6y - 128)x^3 + (y^2 - 8y + 109)x^2 + (6y - 42)x.$

Example 4:

$$\boldsymbol{x}(t) = (t^8 - 8t^6 + 20t^4 - 16t^2 + 2, t^7 - 7t^5 + 14t^3 - 7t),$$
$$\Pi(x, y) = \left(\frac{(x + y + 1)x}{2x^2 + 2y^2 + 2x + 2y + 1}, \frac{(x - y)x}{2x^2 + 2y^2 + 2x + 2y + 1}\right).$$

Example 5:

$$\boldsymbol{x}(t) = \left(\frac{18t^4 + 21t^3 - 7t - 2}{18t^4 + 48t^3 + 64t^2 + 40t + 9}, \frac{36t^4 + 84t^3 + 73t^2 + 28t + 4}{18t^4 + 48t^3 + 64t^2 + 40t + 9}\right),$$
$$\Pi(x, y) = (\Pi_1(x, y), \Pi_2(x, y)),$$
$$\Pi_1(x, y) = \frac{-x^2 - y^2 - 2x}{x^2 + y^2 - x},$$
$$\Pi_2(x, y) = \frac{x^8 + 4x^6y^2 + 6x^4y^4 + 4x^2y^6 + y^8 - x^5y - 2x^3y^3 - xy^5 + x^4 - 2x^3y}{(2x^6 + 6x^4y^2 + 6x^2y^4 + 2y^6 - 2x^5 - 4x^3y^2 - 2xy^4 + x^2y)(x^2 + y^2)}.$$

Example 6:

$$\boldsymbol{x}(t) = (x(t), y(t)), \Pi(x, y) = (\Pi_1(x, y), \Pi_2(x, y))$$
$$x(t) = \frac{\left(14520t^5 - 34100t^4 + 25200t^3 - 6200t^2 + 600t - 20\right)t}{226981t^6 - 133956t^5 + 37515t^4 - 6120t^3 + 615t^2 - 36t + 1},$$
$$y(t) = -\frac{\left(79200t^4 - 112800t^3 + 38200t^2 - 4800t + 200\right)t^2}{226981t^6 - 133956t^5 + 37515t^4 - 6120t^3 + 615t^2 - 36t + 1},$$
$$\Pi_1(x, y) = \frac{3x^2 + 3y^2 + 2x - 5}{4x - 4}, \ \Pi_2(x, y) = \frac{C(x, y)}{D(x, y)},$$
$C(x, y) = -x^8 - 4x^6y^2 - 6x^4y^4 - 4x^2y^6 - y^8 + 6x^6y + 18x^4y^3 + 18x^2y^5 + 6y^7 - 20x^6 + 20x^5y - 36x^4y^2 + 40x^3y^3 - 12x^2y^4 + 20xy^5 + 4y^6 + 48x^5 + 2x^4y + 96x^3y^2 - 36x^2y^3 + 48xy^4 - 38y^5 + 2x^4 - 72x^3y - 12x^2y^2 - 120xy^3 - 30y^4 - 32x^3 - 86x^2y - 96xy^2 + 98y^3 - 68x^2 + 244xy + 52y^2 + 112x - 114y - 41,$

$D(x, y) = \left(x^2 + y^2 - 2x + 1\right)\left(4x^5 - 2x^4y + 8x^3y^2 - 4x^2y^3 + 40x^3 + 24xy^2 - 2y^5 - 20x^4 + 4xy^4 - 8x^3y - 24x^2y^2 - 8xy^3 - 4y^4 + 4x^2y + 12y^3 - 40x^2 + 24xy - 8y^2 + 20x - 18y - 4\right)$

Example 7:

$$\boldsymbol{x}(t) = (t^8 - 8t^6 + 20t^4 - 16t^2 + 2, t^7 - 7t^5 + 14t^3 - 7t),$$
$$\Pi(x, y) = \left(\frac{-x^2 - y^2 + 2x + 4y - 1}{5x^2 + 5y^2 + 2x - 4y + 1}, \frac{2x^2 + 4x + 2(y - 1)^2}{5x^2 + 5y^2 + 2x - 4y + 1}\right).$$

Non-rational curves: (Fig. 6 in Subsection 4.2).

Example 8:

$$\boldsymbol{x}(t) = \left(t, e^t\right), \ \Pi(x, y) = \left(\frac{(x + y + 1)x}{2x^2 + 2y^2 + 2x + 2y + 1}, \frac{(x - y)x}{2x^2 + 2y^2 + 2x + 2y + 1}\right).$$

Example 9:

$$\boldsymbol{x}(t) = \left(t, \frac{t^3 - e^t}{\log(t)}\right), \ \Pi(x, y) = \left(\frac{(x + y + 1)x}{2x^2 + 2y^2 + 2x + 2y + 1}, \frac{(x - y)x}{2x^2 + 2y^2 + 2x + 2y + 1}\right).$$

Example 10:

$$\boldsymbol{x}(t) = \left(t, e^t\right), \ \Pi(x, y) = (\Pi_1(x, y), \Pi_2(x, y)),$$
$$\Pi_1(x, y) = \frac{-x^2 - y^2 - 2x}{x^2 + y^2 - x},$$

$$\Pi_2(x,y) = \frac{x^8+4x^6y^2+6x^4y^4+4x^2y^6+y^8-x^5y-2x^3y^3-xy^5+x^4-2x^3y}{(2x^6+6x^4y^2+6x^2y^4+2y^6-2x^5-4x^3y^2-2xy^4+x^2y)(x^2+y^2)}.$$

Example 11:

$$\boldsymbol{x}(t) = \left(t, \frac{t^3-e^t}{\log(t)}\right), \ \Pi(x,y) = (\Pi_1(x,y), \Pi_2(x,y)),$$

$$\Pi_1(x,y) = \frac{-x^2-y^2-2x}{x^2+y^2-x},$$

$$\Pi_2(x,y) = \frac{x^8+4x^6y^2+6x^4y^4+4x^2y^6+y^8-x^5y-2x^3y^3-xy^5+x^4-2x^3y}{(2x^6+6x^4y^2+6x^2y^4+2y^6-2x^5-4x^3y^2-2xy^4+x^2y)(x^2+y^2)}.$$

Example 12:

$$\boldsymbol{x}(t) = \left(t, e^t\right), \ \Pi(x,y) = \left(1+\frac{4(x-1)}{(x-1)^2+y^2}, \frac{4y}{(x-1)^2+y^2}\right).$$

Example 13:

$$\boldsymbol{x}(t) = \left(t, \frac{t^3-e^t}{\log(t)}\right), \ \Pi(x,y) = \left(1+\frac{4(x-1)}{(x-1)^2+y^2}, \frac{4y}{(x-1)^2+y^2}\right).$$

References

Alcázar, J.G., Díaz Toca, G.M., 2010. Topology of 2D and 3D rational curves. Comput. Aided Geom. Des. 27, 483–502.

Arnon, D., MacCallum, S., 1988. A polynomial time algorithm for the topology type of a real algebraic curve. J. Symb. Comput. 5, 213–236.

Alcázar, J.G., Caravantes, J., Díaz Toca, G.M., Tsigaridas, E., 2020. Computing the topology of a plane or space hyperelliptic curve. Comput. Aided Geom. Des. 78, 101830.

Berberich, E., Emeliyanenko, P., Kobel, A., Sagraloff, M., 2013. Exact symbolic–numeric computation of planar algebraic curves. Theor. Comput. Sci. 491, 1–32.

Cox, D., Little, J., O'Shea, D., 1992. Ideals, Varieties and Algorithms, fourth edition. Springer.

Diatta, D.N., Diatta, S., Rouillier, F., Roy, M.F., Sagraloff, M., 2022. Bounds for polynomials on algebraic numbers and application to curve topology. Discrete Comput. Geom. 67, 631–697.

G.M., Díaz Toca, 2022. http://webs.um.es/gemadiaz/miwiki/doku.php?id=papers.

El Kahoui, M., González-Vega, L., 1996. An improved upper complexity bound for the topology computation of a real algebraic plane curve. J. Complex. 12, 527–544.

González-Vega, L., Necula, I., 2002. Efficient topology determination of implicitly defined algebraic plane curves. Comput. Aided Geom. Des. 19, 719–743.

Hong, H., 1996. An effective method for analyzing the topology of plane real algebraic curves. Math. Comput. Simul. 42, 571–582.

Hudson, H., Reid, M., 2011. Cremona Transformations in the Plane and Space. Cambridge University Press.

Katsamaki, C., Rouillier, F., Tsigaridas, E., Zafeirakopoulos, Z., 2020. On the geometry and the topology of parametric curves. In: Proceedings of the 45th International Symposium on Symbolic and Algebraic Computation (ISSAC 2020). ACM, pp. 281–288.

Mishra, B., 1993. Algorithmic Algebra. Springer.

Mudiyanselage, N.H., Moroz, G., Pouget, M., 2022. Fast high-resolution drawing of algebraic curves. In: Proceedings. ISSAC 2022.

Pérez-Díaz, S., Schicho, J., Sendra, J.R., 2002. Properness and inversion of rational parametrizations of surfaces. Appl. Algebra Eng. Commun. Comput. 13, 29–51.

Strzebónski, A., 2012. Real root isolation for exp-log-arctan functions. J. Symb. Comput. 47, 282–314.